

Reflection and transmission Raman spectroscopy for the chemical characterization of solid materials

E. Ostertag¹, D. Oelkrug² and R. W. Kessler¹

¹ Process Analysis and Technology, Reutlingen Research Institute,
Reutlingen University, D-72762 Reutlingen

² Institute of Physical and Theoretical Chemistry,
University of Tübingen, D-72076 Tübingen

Abstract This paper compares Raman intensities from reflection (X_R) and transmission (X_T) setups for the chemical characterization of solid materials. The suitability of measuring the Raman radiation for deep probing of the inner volume of turbid matter is discussed from a theoretical and an experimental point of view.

1 Introduction to Raman spectroscopy in turbid matter

Raman radiation (RR) originates in the volume of a material mainly from multiple scattered primary radiation, and the Raman signal itself is also elastically scattered many times before it leaves the sample. Figure 6.1 illustrates the generation of RR: A laser irradiates the scattering sample. Photons migrate into the sample and move within the sample a short or long way depending on the scattering and absorption properties of the material. Photons leave the sample with the same wavelength like the laser source as reflected or transmitted primary light. In the case of a Raman scattering event, the RR can be collected in reflection or transmission. RR is a volume effect, where the light is generated in the sample as follow-up process: the longer the light lasts in the sample, the more Raman scattering is generated. Thus even in thick samples measurable Raman transmission intensities can be achieved in a conventional setup.

There is a rising demand for optical analytical techniques which allow a deep probing of solid matter [1, 2]. Transmission Raman spectroscopy has been presented as an emerging tool to gather information

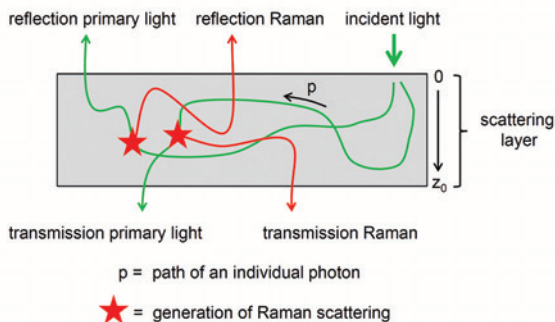


Figure 6.1: Generation of Raman radiation in reflection (X_R) and in transmission (X_T) in a scattering solid sample of layer thickness z_0 . A laser irradiates the sample with a certain number of photons which migrate through the sample, generating Raman photons or leaving the sample as primary light in reflection or transmission.

from the inner volume of solid samples including a quantitative analysis [3,4]. Application examples are in-line process monitoring, fast quality control in pharmaceutical production, counterfeit detection of tablets through the packaging, in-situ characterization of surface reactions on supported catalysts or medical screenings like the noninvasive characterization of tissues and bones. Transmission Raman spectroscopy has already been shown in combination with multivariate data analysis for the quantification of active pharmaceutical ingredients (API) in pharmaceutical mixtures.

Conventional backscattering (= reflection) Raman spectroscopy of opaque media with a low absorption ($\kappa = 0.1$) is strongly biased to the surface layers of the sample from some micrometers up to several millimeters depth [3].

Spatially offset Raman spectroscopy (SORS) marks an approach to overcome the sub-sampling restrictions of conventional backscattering Raman spectroscopy and provides an access to deeper volumes of the sample. Here, the detection is laterally separated with an offset to the laser excitation. Raman spectra can be extracted in combination with multivariate data analysis from different depths of turbid samples [5].

In thin samples with typical thicknesses of $z_0 \leq 1$ cm, the backscat-

tering mode can be expanded by forward scattering (= transmission) Raman spectroscopy. This type of detection was worked out already in 1967 by Schrader and Bergmann [6] and received its revival in 2006 by Matousek and Parker [7]. Hence, transmission Raman spectroscopy represents a special case of SORS for deep Raman probing. Matousek et al [7]. showed for the first time with numerical simulations and experimentally that the depth of impurities in tablets plays a minor role in Raman transmission spectroscopy compared to a Raman backscattering setup, where they are not detected.

2 Model calculation

2.1 Mean path lengths of radiation in a non-absorbing scattering layer

Figure 6.2 depicts the calculated mean path lengths of radiation until reflection $\langle p_R \rangle$ (left) and until transmission $\langle p_T \rangle$ (right) under the assumption of a non-absorbing sample. The calculations are performed with the help of a random walk approach. For the reflection case

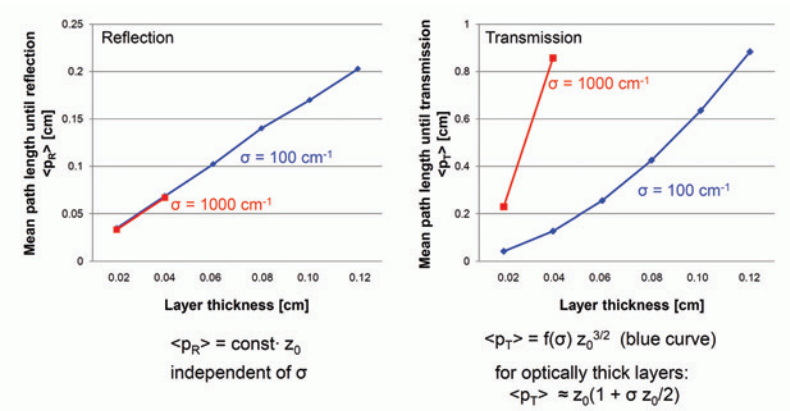


Figure 6.2: Mean path lengths of radiation in a non-absorbing scattering layer calculated by the random walk approach for a reflection (left) and a transmission setup (right).

$\langle p_R \rangle$ is linearly dependent on the layer thickness z_0 and independent of the scattering coefficient σ . For the transmission case the right graph of Fig. 6.2 shows clearly the influence of the scattering coefficient on the mean path length. The figure also indicates the equations for the scattering coefficient $\sigma = 100 \text{ cm}^{-1}$ and for optically thick layers.

2.2 Reflection Raman versus transmission Raman: Monte Carlo simulations

Monte Carlo simulations for calculating the reflected and transmitted Raman intensities of non absorbing and absorbing materials as function of the layer thickness are performed. Figure 6.3 (left) shows, that in strongly scattering media with no absorption the Raman intensity increases with the layer thickness. The reflected Raman intensity is twice the transmitted Raman intensity. In strongly scattering media with absorption (Fig. 6.3, right) Raman backscattering setups yield higher intensities and smaller signal variations due to the smaller Raman active volume element. The presence of sample absorption leads to a decay of the Raman intensities, which is more pronounced in the transmission setup.

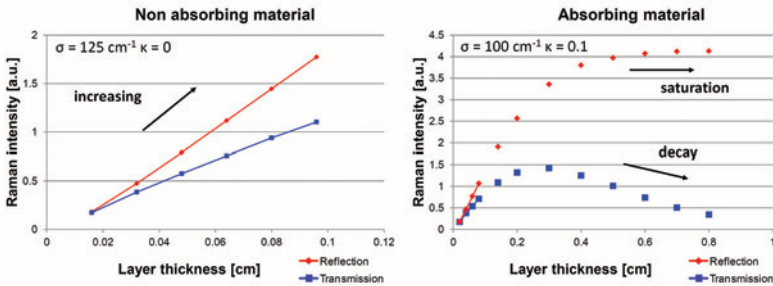


Figure 6.3: Monte Carlo simulations calculate the reflected and transmitted Raman intensities of strongly scattering materials for the cases with no absorption (left) and absorption (right).

3 Measurement setup

The reflection and transmission Raman measurements are carried out with a RamanRXN1TM analyzer from Kaiser Optical Systems, Ann Arbor, USA equipped with an InvictusTM 785 nm NIR diode laser specified for a maximum output power of 450 mW. The spectral resolution is 0.3 cm^{-1} . The laser irradiates the sample via an optical fiber with additional optics. Figure 6.4 illustrates the reflection and transmission setups. For the reflection setup a PhATTM probe is attached to the optical fiber to illuminate the sample with a spot diameter of 0.6 cm. For the transmission setup a transmission illuminator is coupled to the optical fiber for the excitation of the sample with an irradiation diameter of 0.1 cm. The detection is realized for both the reflection and transmission setups with the PhATTM probe with a collection spot diameter of 0.6 cm. The collected Raman and primary radiation passes a further optical fiber and filter elements on the way to the volume phase transmission grating and the Peltier cooled CCD matrix detector to generate the Raman spectra. The Raman intensities X_R and X_T in reflection and transmission are calibrated with liquid cyclohexane in a thin optical cuvette. PTFE as optical diffuse material for thickness dependent investigations is supplied by Gigahertz-Optik, Türkenfeld, Germany in thicknesses of 0.02 and 0.15 cm. Additional thicknesses up to 0.5 cm were cut from a PTFE block or prepared as stacks from the 0.02 cm layer. Cellulose is purchased as filters type MN 615 from Macherey-Nagel, Düren, Germany with 0.016 cm thickness. Acetylsalicylic acid (ASA), product no. 158185000 from Acros Organics, Geel, Belgium is used to press a cylindrical disc with 2 cm diameter and 0.425 cm thickness as inner layer of a composite triple layer. The upper and the lower layer consists of a PTFE layer.

4 Results and discussion

Raman emission in a scattering layer system originates from different depths depending on the reflection or transmission setup. Experiments with multiple, double and triple layer systems illustrate the behavior in z-axis.

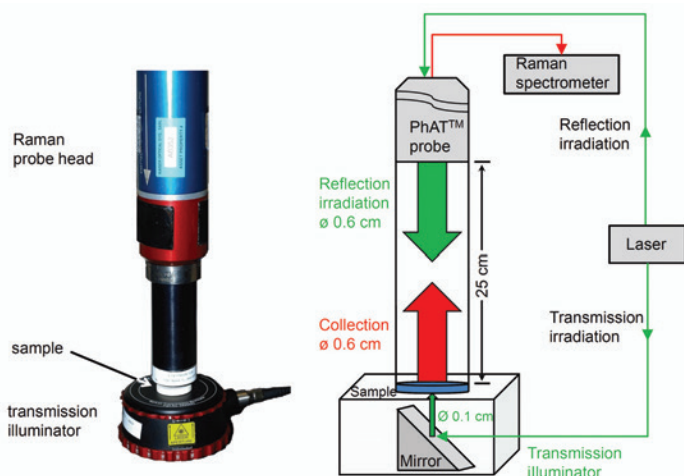


Figure 6.4: Setups for reflection and transmission Raman spectroscopy. In the reflection mode the sample is irradiated from top with a diameter of 0.6 cm (wide area illumination). In the transmission setup the sample is irradiated from the bottom side via the transmission illuminator which generates a spot size diameter of 0.1 cm. The Raman probe head (PhAT™) collects the Raman radiation in both setups with a diameter of 0.6 cm and routes it to the spectrometer. Left: photograph, right: schematic diagram.

4.1 Multiple layer system

Multiple layers with 1 to 5 layers of cellulose and PTFE with both low absorption coefficients are investigated in the reflection and transmission mode (Fig. 6.5). For cellulose the intensities of the Raman band at $\Delta\nu = 1095 \text{ cm}^{-1}$ are recorded at layer thicknesses from 0.016 cm to 0.08 cm in reflection and transmission. The Raman band belongs to several closely spaced intense bands in the region between $\Delta\nu = 950 \text{ cm}^{-1}$ to 1180 cm^{-1} . For PTFE the intensities of the Raman band at $\Delta\nu = 1382 \text{ cm}^{-1}$ are recorded at layer thicknesses from 0.15 cm to 0.5 cm in reflection and transmission. The Raman band at $\Delta\nu = 1382 \text{ cm}^{-1}$ is the most intense sub-band of the characteristic PTFE-triplet. The measured Raman intensities in reflection and transmission of the cellulose multilayer system confirm the Monte Carlo model calculations:

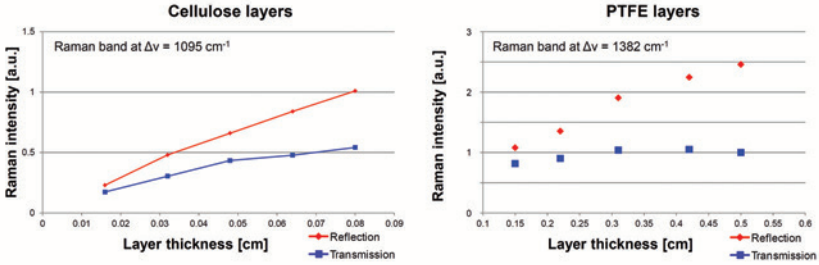


Figure 6.5: Raman intensities in the reflection and the transmission mode from a multilayer system of 1-5 layers of cellulose with low absorption coefficients. The experimental data confirm the results from the Monte Carlo simulations (left). Raman intensities in the reflection and the transmission mode of PTFE with low absorption coefficients at 5 different layer thicknesses show deviations to the model (right).

In strongly scattering media with negligible background absorption the Raman intensity increases with the layer thickness. Here the reflected Raman intensity is twice the transmitted Raman intensity.

In the case of the PTFE system the experimental data show deviations to the model: With a layer thickness above 0.3 cm the transmitted Raman intensity reaches a maximum and then slowly decreases. This behavior may be caused by an unexpected absorption of the layers due to contamination, a too simple model or a limited detection aperture. If a specific layer thickness is reached the Raman photons laterally spread wider than the diameter of the detection area. In the experiments the maximum thickness of the PTFE layers with 0.5 cm exceeds the maximum thickness of the cellulose layers with 0.08 cm by a factor of approximately 6.

4.2 Double layer system

A double layer with two axially separated different Raman emitters A and B produce signals that do not depend only on the thickness of the emitting layer but also on the thickness and position of the co-layer. The reflected Raman intensity X_R of the front layer increases strongly with the thickness of the back layer because part of the initially transmitted

Raman signal is now reflected, but mainly because the density of the primary radiation becomes higher. The reflected intensity of the back layer behaves in the opposite way.

In the experiment in reflection geometry (Fig. 6.6, left) a double layer of cellulose and PTFE is irradiated alternatively from one of the two sides. The PTFE signal from the front side is approximately four times as high as from the back side (see e.g. the Raman band of PTFE at $\Delta\nu = 1382\text{ cm}^{-1}$).

Contrary to X_R , transmission Raman spectra are expected to be independent of the side of irradiation. The spectra of Fig. 6.6 prove experimentally the independency of the side of irradiation in transmission geometry with a double layer of PTFE and cellulose.

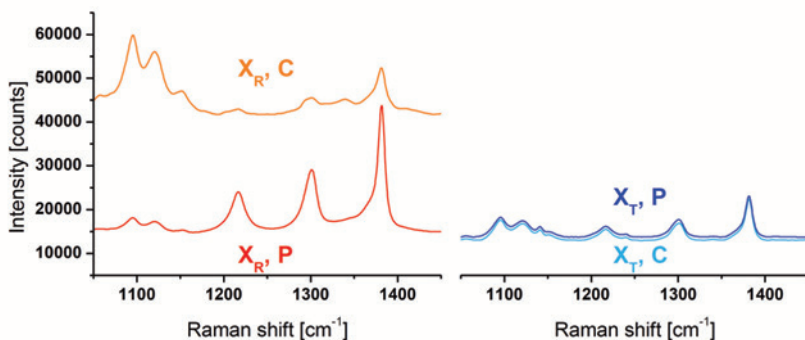


Figure 6.6: Raman reflection and transmission intensities X_R (left) and X_T (right) of a double layer of 0.020 cm PTFE and 0.016 cm cellulose with P = orientation of PTFE to the detector and C = orientation of cellulose to the detector. The spectra are fluorescence corrected. In reflection the measured spectra depend strongly on the upper material. The spectral influence of the subjacent material is lower. In transmission the spectra are independent from the orientation of the layers.

4.3 Triple layer system

A triple layer A/B/A simulates coated tablets or encapsulated powders, and is expected to behave as follows: The reflection mode highlights the

spectrum of A, whereas the transmission mode highlights the spectrum of B since the generation probability of the central layer is much higher than of the border layers.

Figure 6.7 shows experimental data for a triple layer arrangement of PTFE (0.15 cm) / acetylsalicylic acid (ASA, 0.425 cm) / PTFE (0.15 cm). The Raman band at $\Delta\nu = 733\text{ cm}^{-1}$ originates from PTFE, the three other bands from ASA. The Raman reflection setup emphasizes clearly the spectrum of PTFE, the transmission setup the spectrum of ASA.

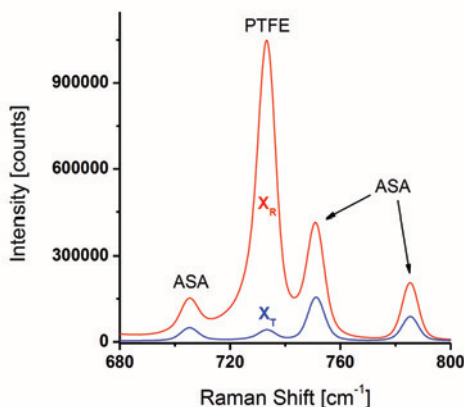


Figure 6.7: Raman reflection (X_R) and transmission intensities (X_T) from a model system of a coated tablet with excess coating thickness (PTFE 0.15 cm / ASA 0.425 cm / PTFE 0.15 cm). In Raman transmission the main spectral information is generated in the inner medium. The band at 733 cm^{-1} Raman shift results from PTFE. The remaining bands are assigned to acetylsalicylic acid. The Raman spectrum of ASA does not comprise a band at $\Delta\nu = 733\text{ cm}^{-1}$.

5 Conclusions and outlook

Reflection Raman spectroscopy yields higher signal intensities than transmission, but is limited in conventional spectroscopy setups to the material located in vicinity to the surface. Nevertheless, the transmission Raman intensities are higher than expected as long as the sample is

not absorbing (X_T is at least half as intense as X_R). In transmission Raman spectroscopy of absorbing samples, the intensity firstly reaches a maximum with increasing layer thickness and then decays. The strong decrease of X_T with absorption is a consequence of the long path length of the transmitted radiation. In those cases the reflection mode is superior to the transmission mode. In solid samples with axial concentration the mean reflected signal originates from the first quarter of the layer depth, whereas the mean transmitted signal originates predominantly from the central regions. Here, for probing the inner volume of a sample the T-mode is superior to the R-mode. As a consequence it must be carefully considered which multilayer systems are measured.

A possible limitation of the detector aperture has to be taken into account as the radial expansion of the signals increases linearly with the layer thickness, where X_T spreads wider than X_R . Especially quantitative transmission Raman spectroscopy requires diameters of the detected sample areas that are adopted thoroughly to the sample thickness.

For an improved detection of buried layers the weak signal strength of transmitted Raman radiation can be enhanced by a dielectric mirror system [8]. In future work the authors will present a modified approach for enhanced reflection Raman spectroscopy, where it is possible to monitor the whole depth of a multiple scattering sample with equal statistical weight. The authors consider an enhanced reflection setup as a favorable approach for inline Raman spectroscopy in process analytical technology.

Acknowledgement

We acknowledge the support of Kaiser Optical Systems Inc. for the allocation of an RXN1TM system.

References

1. R. W. Kessler, *Prozessanalytik - Strategien und Fallbeispiele aus der industriellen Praxis*. Weinheim: Wiley-VCH, 2006.
2. K. A. Bakeev, *Process Analytical Technology - Spectroscopic Tools and Implemen-*

- tation Strategies for the Chemical and Pharmaceutical Industries*, second edition. 2. ed. Chichester: John Wiley and Sons, 2010.
3. K. Buckley and P. Matousek, "Non-invasive analysis of turbid samples using deep Raman spectroscopy," *Analyst*, vol. 136, pp. 3039–3050, 2011.
 4. M. D. Hargreaves, N. A. MacLeod, M. R. Smith, D. Andrews, S. V. Hammond, and P. Matousek, "Characterization of transmission Raman spectroscopy for rapid quantitative analysis of intact multi-component pharmaceutical capsules," *Journal of Pharmaceutical and Biomedical Analysis*, vol. 54, pp. 463–468, 2011.
 5. P. Matousek, I. P. Clark, E. R. C. Draper, M. D. Morris, A. E. Goodship, N. Everall, M. Towrie, W. F. Finney, and A. W. Parker, "Subsurface probing in diffusely scattering media using spatially offset Raman spectroscopy," *Applied Spectroscopy*, vol. 59, pp. 393–400, 2005.
 6. G. Schrader, B.; Bergmann, "Die Intensität des Ramanspektrums polykristalliner Substanzen," *Fresenius' Journal of Analytical Chemistry*, vol. 225, pp. 230–247, 1967.
 7. A. W. Matousek, P.; Parker, "Bulk Raman analysis of pharmaceutical tablets," *Applied Spectroscopy*, vol. 60, pp. 1353–1357, 2006.
 8. P. Matousek, "Raman signal enhancement in deep spectroscopy of turbid media," *Applied Spectroscopy*, vol. 60, pp. 845–854, 2007.